Lower Extremity Reconstruction with Anterolateral Thigh Free-Flap Anastomoses: A Computational Fluid Dynamic Analysis

Sanjay K.A. Jinka, MD[1] Ashoka G.K. Jinka, PhD[2] Jeffrey E. Janis, MD, FACS[3]

[1] College of Medicine, Northeast Ohio Medical University, Rootstown, Ohio
[2] Independent Computational Modeling Consultant, Maumee, Ohio
[3] Department of Plastic and Reconstructive Surgery, Ohio State University Wexner Medical Center, Columbus, Ohio

Address for correspondence Jeffrey E. Janis, MD, FACS, Ohio State University Wexner Medical Center, 915 Olentangy River Road, Suite 2100, Columbus, OH 43212 (e-mail: Jeffrey.Janis@osumc.edu).

J Reconstr Microsurg

Abstract

Background The anterolateral thigh free flap is an option for repairing soft tissue defects of the distal lower extremity. This flap uses the descending branch of the lateral circumflex femoral (LCF) artery as the flap vessel. The recipient vessel in these flaps is often the anterior tibial (AT), posterior tibial (PT), or peroneal (P) arteries. Computational fluid dynamic (CFD) evaluation of anastomoses between these vessels can optimize outcomes.

Methods Thirty-eight CFD models were created to model end-to-side (ETS) and end-to-end (ETE) anastomoses for lower extremity reconstruction. Seven out of thirty-eight models represented ETS anastomoses between the LCF and AT arteries with varying anastomotic angles. Nine out of thirty-eight models represented 45-degree ETS anastomoses between varying diameters of the LCF and AT, PT, and P arteries. Nine out of thirty-eight models represented stenosis on the flap vessel and recipient vessel, pre- and post-bifurcation. Nine out of thirty-eight models represented ETE anastomoses, rather than ETS, with varying vessel diameters. Four out of thirty-eight models represented ETE anastomoses with varying regions and levels of stenosis.

Results Stasis of blood flow in ETS models increased as anastomotic angle increased in a logarithmic relationship ($R^2 = 0.918$). Flow was optimized overall as flap and recipient vessel diameters approached one another. In ETS models, flap vessel and postbifurcation recipient vessel stenosis were found to substantially increase stasis.

Conclusion Selection of flap and recipient vessels with similar diameters can optimize outcomes in microvascular anastomoses. In the context of lower extremity reconstruction with the ALT flap, the PT artery can be recommended as a first-line recipient vessel due to its similar vessel caliber to the LCF and relative ease of surgical access compared with the P artery. Avoidance of areas of stenosis is recommended to ensure laminar flow and reduce the operative difficulty associated with performing anastomoses on nonpliable arteries. Striving for increased acuity of anastomotic angles is recommended to optimize the flow in ETS microvascular anastomoses.

Keywords
- lower extremity reconstruction
- anterolateral thigh free flap
- microvascular anastomoses
- computational fluid dynamics
- end-to-side
- end-to-end

received
July 28, 2022
accepted after revision
February 28, 2023
accepted manuscript online
March 16, 2023

Thieme Medical Publishers, Inc.,
333 Seventh Avenue, 18th Floor,
New York, NY 10001, USA

DOI https://doi.org/10.1055/a-2056-0629.
ISSN 0743-684X.

Introduction

Reconstruction of complex lower limb defects can be challenging, oftentimes requiring microvascular free tissue transfer.[1] The anterolateral thigh flap, based on the descending branch of the lateral circumflex femoral (LCF) artery, represents a reconstructive solution for moderate-to-large soft-tissue defects.[2,3] The end-to-side (ETS) anastomosis technique to the anterior tibial (AT), posterior tibial (PT), or peroneal arteries (P) is often used in these procedures to preserve distal extremity perfusion.[2–7] Understanding how differences in these vessels' diameters affect blood stasis is important for selecting an artery for the procedure.

Another consideration for free tissue transfers is atherosclerosis.[8–12] This is especially a concern in lower extremity reconstruction where distal segments of the lower limb have been noted to have severe stenosis in at-risk populations.[13,14]

To date, no computational fluid dynamic (CFD) studies have been conducted regarding the anterolateral thigh free flap in a lower-extremity model, which can be used to optimize flow across the anastomosis. This study creates CFD models for an ETS and end-to-end (ETE) anterolateral thigh free flap from the LCF to the AT, PT, and P arteries to determine what characteristics optimize blood flow. Simulations with various levels of stenosis at multiple points in the AT/LCF anastomotic model were also created to help determine what degree and location(s) of stenosis may be concerns for the procedure.

Methods

In total, 38 models (25 ETS and 13 ETE) were created to better understand lower extremity anastomoses (►**Fig. 1**, ►**Tables 1**–**2**).

End-to-Side Angle Analysis

Seven models with anastomotic angles ranging from 15 to 105 degrees were created to represent ETS anastomoses from the descending branch of the LCF to the AT artery (models 1–7, ►**Table 1**). The LCF artery was defined as the flap vessel and AT artery as the recipient vessel. The lumen diameters of the LCF and AT arteries were 2.0[15] and 3.5[16] mm, respectively.

End-to-Side Vessel Diameter Analysis

Nine models were created to represent ETS anastomoses between the LCF and AT, PT, and P arteries (models 8–16, ►**Table 1**). In these models, the LCF artery was defined as the flap vessel and AT, PT, and P arteries as the recipient vessels. The lumen diameters of the AT, PT, and P arteries were 3.5, 3.1, and 3.0 mm, respectively.[16] Three models were created with each recipient artery (totaling nine models) to assess the effect of varying LCF lumen diameters on these anastomoses. The LCF diameters were defined as 1.5 2.0, and 2.5 mm for each respective model.[15]

End-to-Side Stenosis Analysis

Nine models were created to represent varying levels of stenosis within ETS anastomoses between the LCF and AT arteries (models 17–25, ►**Table 1**). For this analysis, the LCF artery was defined as the flap vessel and AT artery as the recipient vessel. Stenosis was modeled on the recipient artery proximal and distal to the bifurcation. These were designated as pre- and postbifurcation stenosis models, respectively (►**Fig. 2**). Additionally, stenosis was modeled on the flap artery distal to the bifurcation. This was designated as the flap artery stenosis model. The area of stenosis in each model was 10 mm long and 10 mm from the bifurcation.

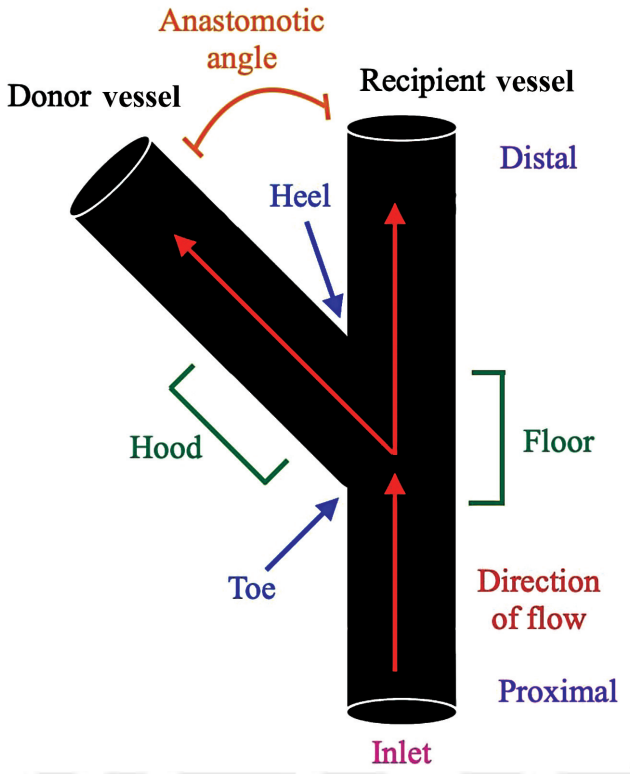

Fig. 1 Anatomy of a microvascular anastomosis.

End-to-End Models

Thirteen models were created to represent an ETE anastomosis between the LCF and AT, PT, and P arteries (models 26–38, ►**Table 2**). Nine models with varying flap/recipient vessel diameters were created. Stenosis was modeled on four LCF to AT models with the area of stenosis in each model being 10 mm long and 10 mm from the bifurcation. Each stenosis model was evaluated with varying regions/percentages of occlusion.

Other Geometric/Flow Conditions

All vessels had 200-micron wall thickness and length of 100 mm.[15] The attachment point of the flap vessel to the recipient vessel in the ETS model was 50 mm distal to the inlet of the recipient vessel.

OpenFOAM v9 was used to create finite volume three-dimensional models and assess fluid flow.[17] Fluid flow in ETS models was evaluated with line integral convolution (LIC) and pure fluid velocity (PFV) modalities. PFV and wall shear stress (WSS) were modeled in ETE models.

Table 1 Computational End-to-Side Models

Model #	Recipient vessel diameter (mm)	Flap vessel diameter (mm)	Anastomotic angle (degrees)	Type of stenosis (if any)	Percent of stenosis
1	3.5	2.0	15	None	N/A
2	3.5	2.0	30	None	N/A
3*	3.5	2.0	45	None	N/A
4	3.5	2.0	60	None	N/A
5	3.5	2.0	75	None	N/A
6	3.5	2.0	90	None	N/A
7	3.5	2.0	105	None	N/A
8	3.5	1.5	45	None	N/A
9*	3.5	2.0	45	None	N/A
10	3.5	2.5	45	None	N/A
11	3.1	1.5	45	None	N/A
12	3.1	2.0	45	None	N/A
13	3.1	2.5	45	None	N/A
14	3.0	1.5	45	None	N/A
15	3.0	2.0	45	None	N/A
16	3.0	2.5	45	None	N/A
17	3.5	2.0	45	Flap artery	25
18	3.5	2.0	45	Flap artery	50
19	3.5	2.0	45	Flap artery	75
20	3.5	2.0	45	Postbifurcation	25
21	3.5	2.0	45	Postbifurcation	50
22	3.5	2.0	45	Postbifurcation	75
23	3.5	2.0	45	Prebifurcation	25
24	3.5	2.0	45	Prebifurcation	50
25	3.5	2.0	45	Prebifurcation	75

*Models 3 and 9 are equivalent.

Table 2 Computational End-to-End Models

Model #	Recipient vessel diameter (mm)	Flap vessel diameter (mm)	Type of stenosis (if any)	Percent of stenosis
26	3.5	1.5	None	N/A
27	3.5	2.0	None	N/A
28	3.5	2.5	None	N/A
29	3.1	1.5	None	N/A
30	3.1	2.0	None	N/A
31	3.1	2.5	None	N/A
32	3.0	1.5	None	N/A
33	3.0	2.0	None	N/A
34	3.0	2.5	None	N/A
35	3.5	2.0	Postanastomosis	25
36	3.5	2.0	Postanastomosis	75
37	3.5	2.0	Preanastomosis	25
38	3.5	2.0	Preanastomosis	75

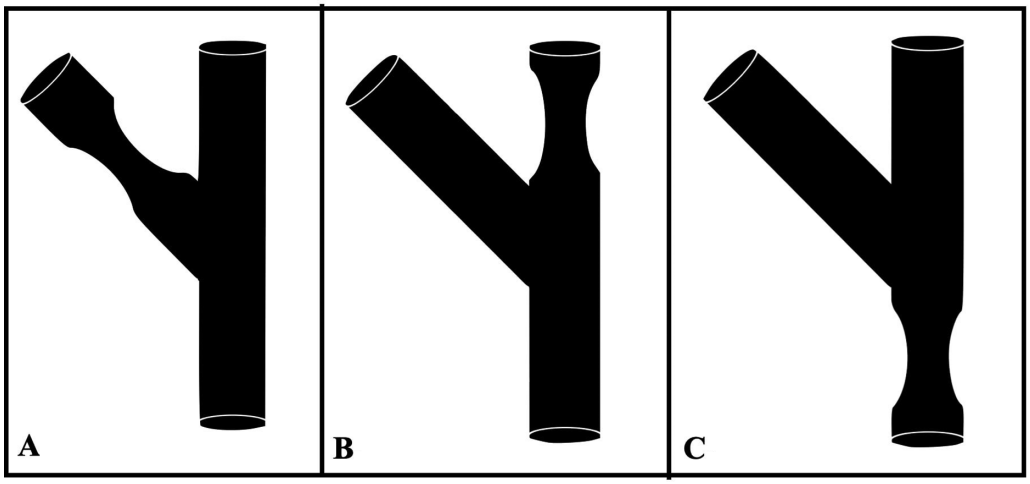

Fig. 2 Types of modeled stenosis. **(A)** Flap artery stenosis. **(B)** Postbifurcation stenosis model. **(C)** Prebifurcation stenosis model.

Blood flow was modeled as an incompressible Newtonian fluid with viscosity (η) of 3.5×10^{-3} Pa·s and density (ρ) of 1,060 kg/m^3.[18,19] Viscosity and density was assumed to be constant throughout the simulation process. Blood flow velocity (μ) at the inlet was defined as 500 mm/s.[20,21]

Validation of Models

The models in this study were not formally validated with subsequent microsurgical in-vivo Doppler testing. However, several considerations were put in place to maximize clinical applicability including using a low tolerance for iterative, temporal, and spatial convergence of 10^{-4}, verifying results are consistent with laws of fluid dynamics and ensuring findings align with other experimental data (as described in the discussion). Taken together, these considerations are in line with the National Program for Applications-Oriented Research in CFD recommendations for controlling uncertainty in CFD simulations and our models may therefore be used to draw clinically applicable conclusions.[22]

Results

End-to-Side Angle Analysis

Our analysis revealed acute anastomotic angles are associated with decreased blood stasis. LIC models of AT and LCF artery anastomoses showed that this stasis was present at the toe of the bifurcation specifically (►**Fig. 3**). This stasis was found to decrease as anastomotic angle decreased (►**Table 3**, ►**Fig. 4**). The relationship between anastomotic angle and maximum cross-sectional stagnation in the flap vessel was found to be logarithmic ($R^2 = 0.918$). Stagnation in these models ranged from 23.00 to 58.90% (with decreased percent stagnation being preferable) in cases with anastomotic angles of 15 and 105 degrees, respectively. PFV simulation revealed the 15-degree model exhibited the highest fluid velocity in the flap vessel.

End-to-Side Vessel Diameter Analysis

Our analysis revealed that anastomoses with vessels of similar diameters are associated with decreased stasis (►**Table 4**, ►**Figs. 5**–**6**). The relationship between flap vessel diameter and maximum cross-sectional stagnation in the flap vessel was found to be strongly linear for all modeled recipient vessels ($R^2 = 0.991$, 1.000, and 0.999 for the AT, PT, and P recipient arteries, respectively).

Further, anastomoses including the P Artery (models 14–16) exhibited the lowest percent stagnation of all modeled flap vessels.

End-to-Side Stenosis Analysis

Our analysis revealed stenosis in the flap vessel can lead to complete blood stasis. LIC models with flap vessel stenosis revealed substantial areas of stagnation at the toe of the bifurcation (►**Fig. 7**). This stagnation was found to decrease as the percentage of stenosis decreased (►**Table 5**, ►**Fig. 8**). Maximum cross-sectional stagnation in the flap vessel ranged from 66.54 to 89.10% for models with 25 and 75% stenosis, respectively. When all other conditions were kept constant, but stenosis was removed, maximum stagnation was reported as 45.49%. The relationship between flap vessel stenosis and maximum cross-sectional stagnation in the flap vessel was found to be strongly linear ($R^2 = 0.973$). PFV analysis went on to show average flow in the model with 75% stenosis approached 0.00 m/s in the flap vessel.

LIC analysis showed that stenosis in the recipient vessel, distal to the site of anastomosis, can improve blood flow to the flap vessel (►**Fig. 9**). Notably, at 75% stenosis, maximum cross-sectional stagnation in the flap vessel approached 0%. PFV analysis of these models showed average flap vessel fluid velocity increased as the percent of stenosis increased.

LIC analysis showed that stenosis in the recipient vessel, proximal to the site of anastomosis, had no clinically appreciable effect on blood flow in the model. Laminar flow was noted throughout the models (►**Fig. 10**). PFV analysis revealed similar velocity of flow in the flap vessels across all prebifurcation stenosis models, irrespective of percent stenosis.

End-to-End Vessel Diameter Analysis

Our analysis revealed that ETE anastomoses with vessels of similar diameters are associated with laminar flow and decreased vessel WSS. Further, ETE models exhibited no

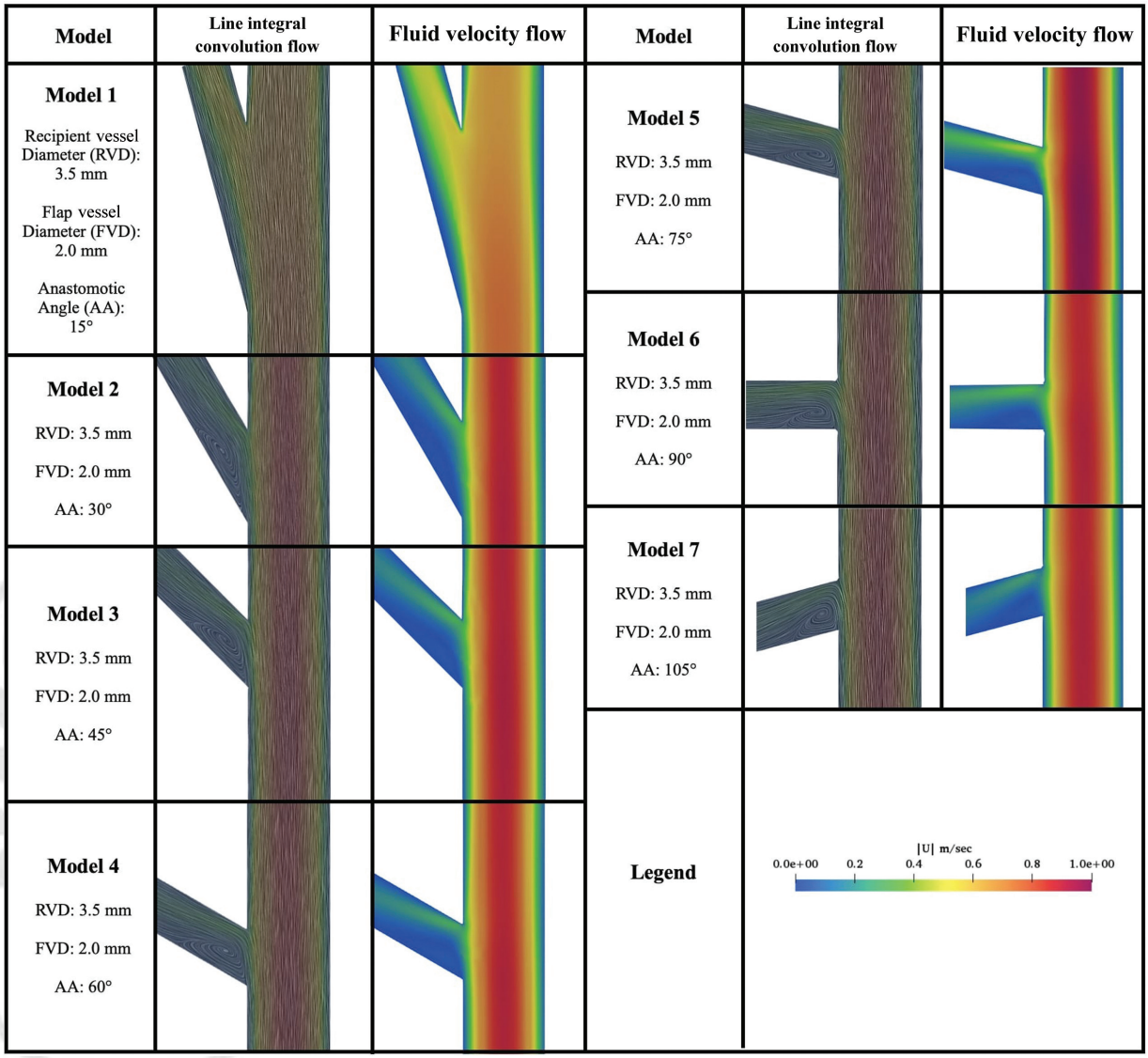

Fig. 3 Effect of anastomotic angle on flow in lower extremity anastomoses.

Table 3 Maximum Percentage of Stagnation in a Lower Extremity CFD Model vs Vessel Angle

Model	Anastomotic angle (degrees)	Maximum stagnation (%)
1	15	23.00
2	30	44.93
3	45	49.49
4	60	52.50
5	75	54.62
6	90	55.88
7	105	58.90

areas of flow stagnation irrespective of vessel diameter (►**Fig. 11**). The greatest point of WSS in these models was at the site of anastomosis.

End-to-End Stenosis Analysis

ETE models with stenosis exhibited no clinically appreciable areas of stasis (►**Fig. 12**). Our analysis revealed that models with stenosis located distal to the anastomosis (models 35 and 36) exhibited no clinically relevant differences in flow or WSS at the site of anastomosis when compared with a simulation without stenosis (model 27, ►**Fig. 11**).

Models with stenosis located proximal to the anastomosis (models 37 and 38) revealed increased WSS and less uniform flow at the site of anastomosis when compared with the model without stenosis (model 27). Further, increased percent occlusion in these stenosis models was associated with increased WSS and flow disturbance.

Discussion

This study is the first to use CFD modeling to understand the mechanics behind lower extremity anastomoses. This is

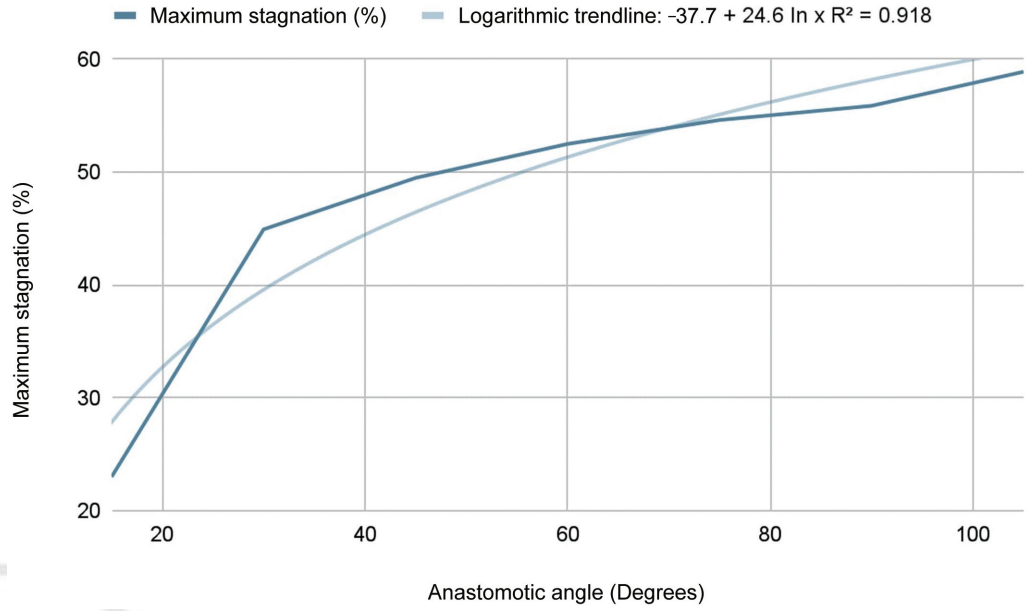

Fig. 4 Stagnation in a lower extremity CFD model versus vessel angle.

Table 4 Maximum Percentage of Stagnation vs Vessel Diameter

Model	Recipient artery	Recipient artery diameter (mm)	Flap vessel diameter (mm)	Maximum stagnation (%)
8	Anterior Tibial	3.5	1.5	55.20
9	Anterior Tibial	3.5	2.0	49.49
10	Anterior Tibial	3.5	2.5	45.41
11	Posterior Tibial	3.1	1.5	50.06
12	Posterior Tibial	3.1	2.0	45.39
13	Posterior Tibial	3.1	2.5	40.98
14	Peroneal	3.0	1.5	48.44
15	Peroneal	3.0	2.0	44.48
16	Peroneal	3.0	2.5	40.06

important as the overall success rate of free-flap procedures in the lower extremity specifically remains lower than head and neck and breast free flaps at 95 versus 98 and 99%, respectively.[23] One of the most common concerns with all anastomoses is thrombosis, a complication with an occurrence rate of 2.3% in a recent retrospective review.[24] Thrombosis may be minimized by optimizing components of Virchow's triad, namely stasis.[25]

Our study found that stasis within lower-extremity ETS anastomoses can be minimized by increasing the acuity of anastomotic angles. This finding was echoed in our previous CFD analysis of ETS anastomoses in the context of DIEP flaps.[26] However, this present study expands upon these findings by including 15- and 105-degree angles. Notably, the relationship between angle and stasis within DIEP flaps was noted to be linear, while this present study revealed a logarithmic relationship. This is most likely the result of adding the 15-degree model which exhibited the lowest stagnation of all models included in this study at 23.00%. This was almost half the stagnation value recorded for the 30-degree AT/LCF artery model (44.93%). This is clinically relevant as it points to the substantial positive effects of minimizing anastomotic angles. However, the difference between a 15- and 30-degree anastomosis, while obvious in a computational simulation, may be difficult to discern in the operating room. These data points were included in the study not to recommend a specific anastomotic angle, but rather to further illustrate the trend that a more acute anastomotic angle results in more laminar flow.[26]

Previous hemodynamic analysis of anastomotic angles in real physical models supports the findings of our computational analysis.[27–29] One study evaluating carotid to carotid ETS anastomoses in a live rat model showed that 56.5% of total carotid flow went through the flap vessel when a 45-degree angle was employed compared with 46.5 and 43.2% for angles of 90- and 135-degrees, respectively.[27] This substantially decreased flow failed to normalize postoperatively, with flow in the 135-degree group dropping to 39.9% 2 hours into the postoperative period. This further highlights the importance of considering more acute anastomotic angles for optimizing ETS flap success.

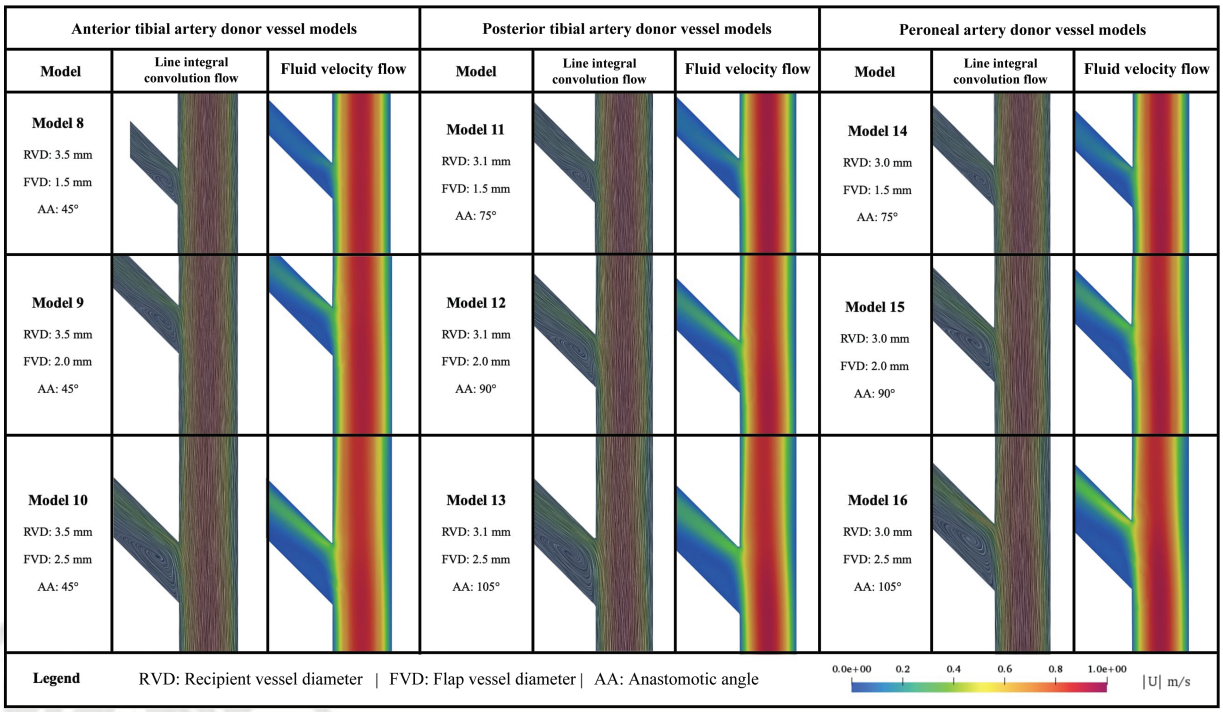

Fig. 5 Effect of vessel diameter on flow in lower extremity anastomoses.

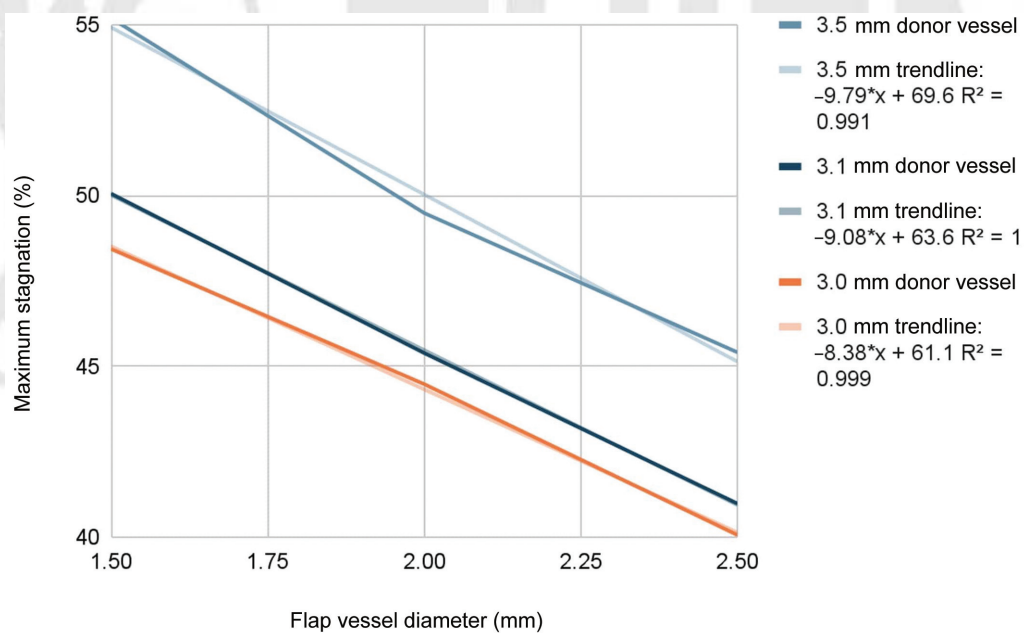

Fig. 6 Stagnation in a lower extremity CFD model versus vessel diameter.

Another factor our study found to affect flow was vessel diameter. As flap vessel diameter approached recipient vessel diameter, flow became more laminar and flap vessel fluid velocity increased in both ETS/ETE models. Further, WSS at the site of anastomosis decreased in ETE models as vessel diameters approached one another. This is clinically significant as WSS and irregular flow are associated with rapid thrombosis, ischemia, and flap failure.[25,30] Further, the importance of selecting vessels with similar diameters has been previously identified in in-vivo rat models.[31,32] One study quoted flap survival in cases with a 2:1 vessel diameter mismatch at 30% compared with 90% survival for flaps with a 1:1 vessel size match.[31]

Intraoperatively, although vessel diameters cannot be intrinsically changed like anastomotic angles, the surgeon can select flap and recipient vessels that closely match in diameter. Our study points to the peroneal artery and descending branch of the LCF artery as one option to optimize for this in lower extremity reconstructions with the anterolateral thigh free flap. While patient arteries may not match the exact dimensions included in this present study, contrast-enhanced magnetic resonance angiography suggests that the P artery

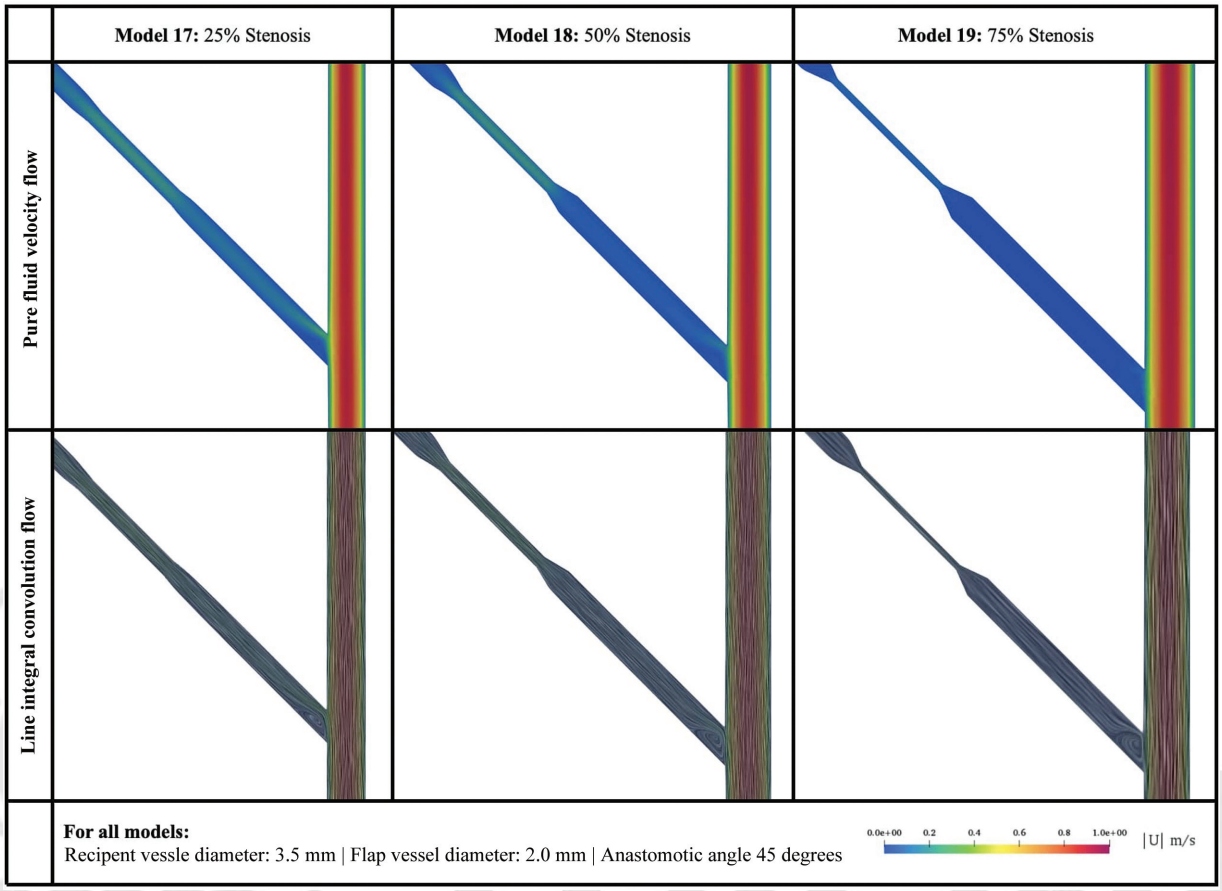

Fig. 7 Effect of flap vessel stenosis on flow in lower extremity anastomoses.

Table 5 Maximum Percentage of Stagnation vs Flap Vessel Stenosis

Model	Percent of Flap vessel stenosed	Maximum stagnation (%)
3/9	0	45.49
17	25	66.54
18	50	76.05
19	75	89.10

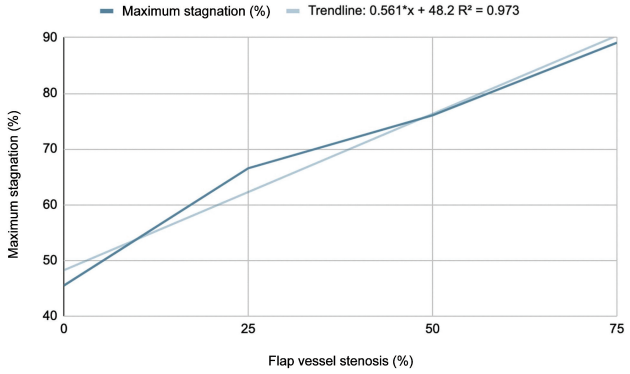

Fig. 8 Stagnation in a lower extremity CFD model versus flap vessel stenosis.

more often approaches the diameter of the LCF when compared with AT and PT arteries.[16] Therefore, the P/LCF artery pair may be worth considering as a first line in anterolateral thigh free-flap reconstructions of the lower extremity.

This being said that there are factors other than the anatomic diameter to consider when choosing a recipient vessel. For example, a previous retrospective review recommended the PT artery over the AT due to a lower incidence of injury and less extensive damage on average following trauma.[33] Further, ease of surgical access is important to consider. The P artery, although hemodynamically ideal, can be challenging to access, often requiring partial fibula resection for adequate exposure.[34,35] Given this, the PT artery may be the overall best option for a recipient vessel that balances surgical access, protection against subsequent injury, and hemodynamic optimization. Despite this recommendation, the selection of recipient vessel ultimately requires surgical clinical decision-making based on the surgeon, patient, and situation-specific factors.

One of these other considerations is stenosis of the vessel. Analysis of the LCF found the lumen diameter was significantly smaller in patients with atherosclerotic risk factors when compared with those without risk factors.[36] Another article evaluating lumen diameters of 70-year-old patients found that the AT artery had an average of 20.5% stenosis.[37]

Our study suggests the position of this stenosis in relation to the site of ETS anastomosis is critical to flap survival. Stenosis within the flap vessel, although not reported commonly in the

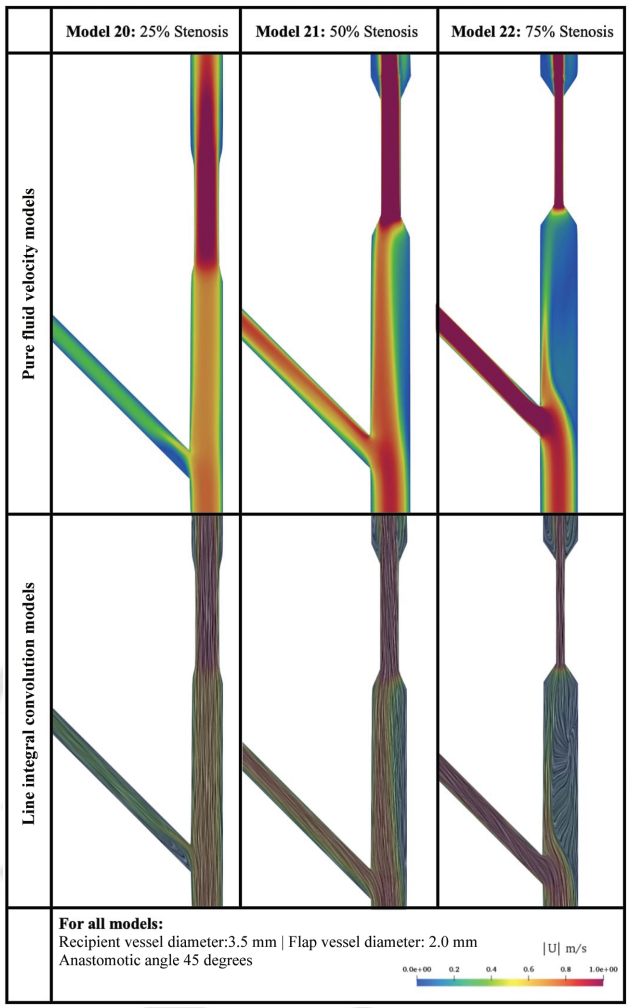

Fig. 9 Effect of postbifurcation vessel stenosis on flow in lower extremity anastomoses.

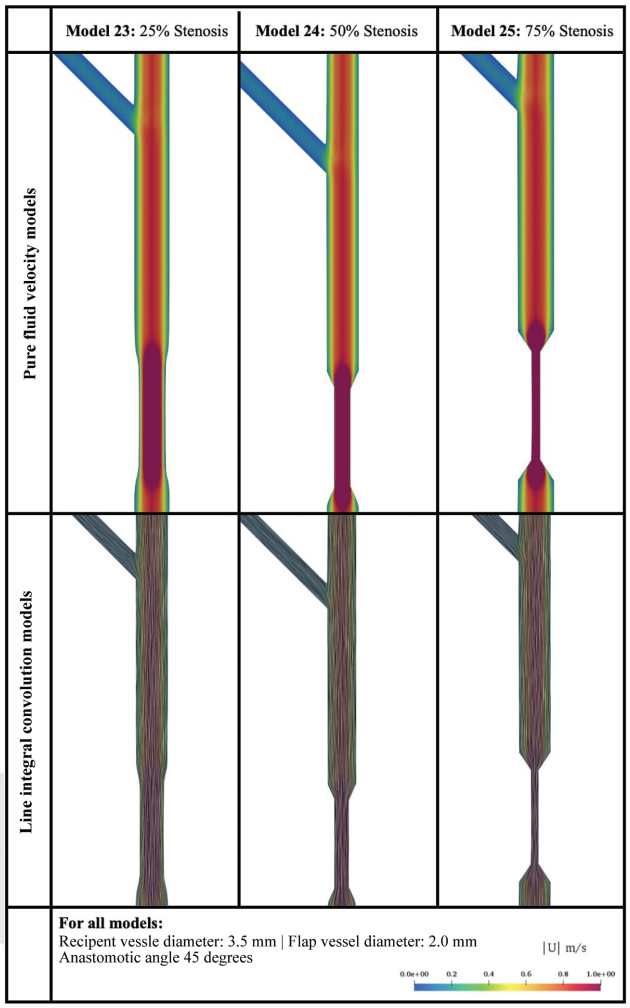

Fig. 10 Effect of prebifurcation vessel stenosis on flow in lower extremity anastomoses.

literature, leads to substantial stasis in ETS anastomoses with one of our models approaching 90 percent stasis. This would likely lead to ischemia or rapid thrombus formation, compromising flap survival. In ETS cases where patients have stenosis in the recipient artery, specifically distal to the planned site of anastomosis, completing the anastomosis may compromise distal blood flow in the recipient artery, eliminating the benefits of an ETS anastomosis. Accordingly, a 2012 study recommends ETE anastomoses in cases where substantial atherosclerotic change is present in the recipient vessel.[38]

When considering stenosis in planned ETE anastomoses our study reveals a similar relationship where blood flow is disturbed and WSS is increased in cases with stenosis distal to the site of anastomosis. This suggests that substantial stenosis in the flap vessel of ETE anastomoses can lead to flap failure.[25,30] This being said, stenosis in the flap vessel already poses a challenge for arterial anastomoses as calcification or radiation-induced fibrosis can make vessels friable and nonpliable, requiring fine microsurgical technique.[8,39] Taken together, we recommend avoiding vessels with significant atherosclerosis/stenosis or performing the anastomosis distal to sites of stenosis.

Previously some surgeons have recommended preoperative CT angiography (CTA) to assess for abnormalities before performing free-flap procedures.[11,36] We feel CTA may be necessary in patients with risk factors, but near-infrared indocyanine-green (ICG) angiography is another option to optimize stenosis-related outcomes intraoperatively.[40] At present atherosclerosis is not a contraindication for lower extremity free-flap reconstruction.[8] Our findings support this guideline as long as the surgeon is mindful of stenosis identified intraoperatively and the associated potential increase in technical microsurgical difficulty. In any case, close monitoring of at-risk patients is highly recommended.

Limitations

The measurements used in our models are based on peer-reviewed averages which may differ from patient to patient. By incorporating a range of vessel diameters, we attempt to address this shortcoming, although patients will inevitably have vessel dimensions that fall outside the scope of the models included in this study. Additionally, this study does not consider the pulsatile nature of blood. Future research may consider this factor to further understand how to optimize anastomoses.

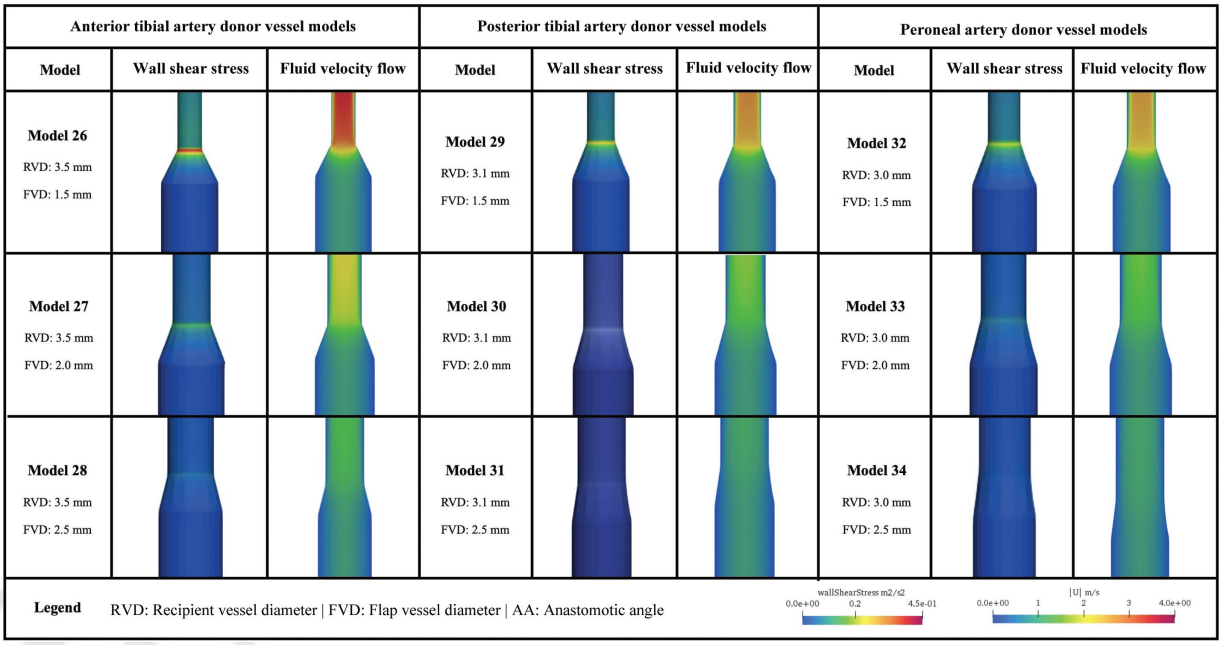

Fig. 11 Effect of vessel diameter on flow and wall shear stress in ETE anastomoses.

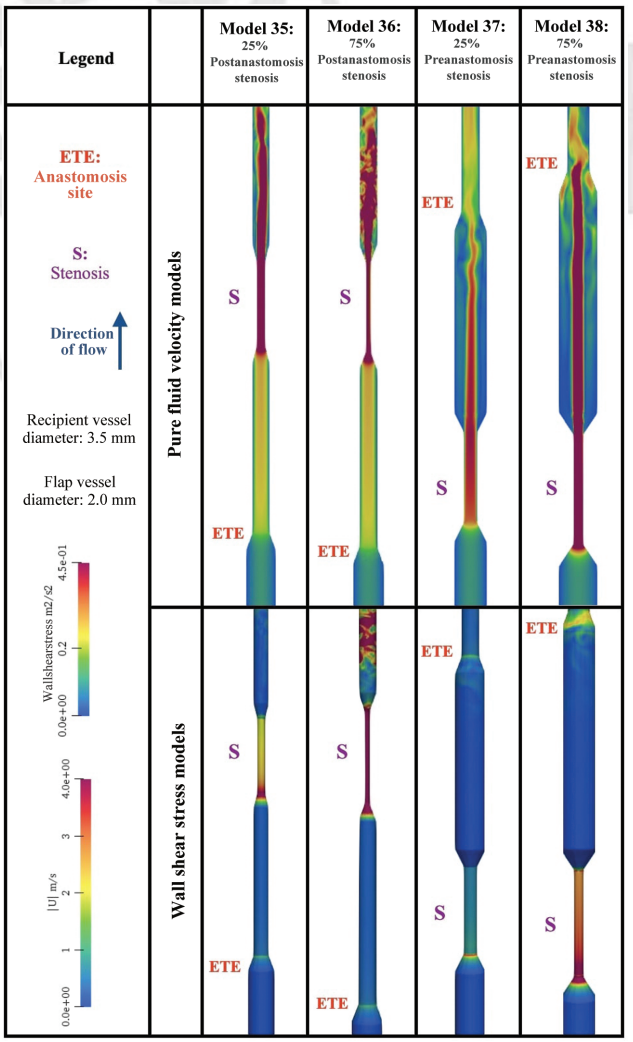

Fig. 12 Effect of vessel stenosis on flow and wall shear stress in end-to-end anastomoses.

Conclusion

CFD evaluation is useful for understanding the physics behind microvascular anastomoses. Striving to create anastomotic angles with increased acuity can decrease the stasis of blood in the flap vessel and may improve ETS flap success. Selection of flap and recipient vessels with similar diameters can further decrease stasis and risk of thrombotic failure in both ETS and ETE flaps. In the context of lower extremity reconstruction with the anterolateral thigh free flap, the posterior tibial artery is a recipient vessel option that strikes a balance between surgical accessibility and most closely matching the vessel diameter of the descending branch of the LCF artery flap vessel. Flap vessels with atherosclerosis/stenosis should be avoided when possible. Recipient vessels with stenosis may be salvaged if the anastomosis is placed distal to the defect and the surgeon is mindful of the possible increase in technical microsurgical difficulty. To best optimize these outcomes, preoperative CTA, intraoperative ICG angiography, and/or close post-operative monitoring should be incorporated into the care of all at-risk patients when performing lower extremity reconstruction with microvascular anastomosis.

Disclosures
J.E.J. receives royalties from Springer Publishing and Thieme Publishers. S.K.A. J. and A.G.K.J. have no financial disclosures.

Funding
None.

Conflict of Interest
None declared.

References

1 Grotting JC, Vasconez LO. Regional blood supply and the selection of flaps for reconstruction. Clin Plast Surg 1986;13(04):581–593
2 Nemoto M, Ishikawa S, Kounoike N, Sugimoto T, Takeda A. Free flap transfer to preserve main arterial flow in early reconstruction of open fracture in the lower extremity. Plast Surg Int 2015; 2015:213892
3 Kang MJ, Chung CH, Chang YJ, Kim KH. Reconstruction of the lower extremity using free flaps. Arch Plast Surg 2013;40(05): 575–583
4 Rossi MJ, Zolper EG, Bekeny JC, et al. Free tissue transfer using end-to-side arterial anastomosis for limb salvage in patients with lower extremity arterial disease. J Vasc Surg 2020;72(01):e268
5 Broer PN, Moellhoff N, Mayer JM, Heidekrueger PI, Ninkovic M, Ehrl D. Comparison of outcomes of end-to-end versus end-to-side anastomoses in lower extremity free flap reconstructions. J Reconstr Microsurg 2020;36(06):432–437
6 Samaha FJ, Oliva A, Buncke GM, Buncke HJ, Siko PP. A clinical study of end-to-end versus end-to-side techniques for microvascular anastomosis. Plast Reconstr Surg 1997;99(04):1109–1111
7 Pederson WC, Grome L. Microsurgical reconstruction of the lower extremity. Semin Plast Surg 2019;33(01):54–58
8 Chen HC, Coskunfirat OK, Özkan O, et al. Guidelines for the optimization of microsurgery in atherosclerotic patients. Microsurgery 2006;26(05):356–362
9 Hage JJ, Woerdeman LAE. Lower limb necrosis after use of the anterolateral thigh free flap: is preoperative angiography indicated? Ann Plast Surg 2004;52(03):315–318
10 Lee YK, Park KY, Koo YT, et al. Analysis of multiple risk factors affecting the result of free flap transfer for necrotising soft tissue defects of the lower extremities in patients with type 2 diabetes mellitus. J Plast Reconstr Aesthet Surg 2014;67(05):624–628
11 Chow LC, Napoli A, Klein MB, Chang J, Rubin GD. Vascular mapping of the leg with multi-detector row CT angiography prior to free-flap transplantation. Radiology 2005;237(01):353–360
12 Serletti JM, Deuber MA, Guidera PM, et al. Atherosclerosis of the lower extremity and free-tissue reconstruction for limb salvage. Plast Reconstr Surg 1995;96(05):1136–1144
13 van der Feen C, Neijens FS, Kanters SDJM, Mali WP, Stolk RP, Banga JD. Angiographic distribution of lower extremity atherosclerosis in patients with and without diabetes. Diabet Med 2002;19(05): 366–370
14 Gallino A, Aboyans V, Diehm C, et al; European Society of Cardiology Working Group on Peripheral Circulation. Non-coronary atherosclerosis. Eur Heart J 2014;35(17):1112–1119
15 Scott Levin L, Baumeister S. Lower extremity. In: Wei FC, Mardini S, eds. Flaps and Reconstructive Surgery. W.B. Saunders; 2009: 63–70
16 Lorbeer R, Grotz A, Dörr M, et al. Reference values of vessel diameters, stenosis prevalence, and arterial variations of the lower limb arteries in a male population sample using contrast-enhanced MR angiography. PLoS One 2018;13(06):e0197559
17 The OpenFOAM Foundation OpenFOAM.; 2021
18 Liu H, Lan L, Abrigo J, et al. Comparison of Newtonian and Non-Newtonian fluid models in blood flow simulation in patients with intracranial arterial stenosis. Front Physiol 2021;12;. Doi: 10.3389/fphys.2021.718540
19 Silva Jde A, Karam-Filho J, Borges CCH. Computational analysis of anastomotic angles by blood flow conditions in side-to-end radiocephalic fistulae used in hemodialysis. J Biomed Sci Eng 2015;8 (03):131–141
20 Wendkos MH, Rossman PL. The normal blood pressure in the lower extremity. Am Heart J 1943;26(05):623–630
21 Sheppard JP, Lacy P, Lewis PS, Martin UBlood Pressure Measurement Working Party of the British and Irish Hypertension Society. Measurement of blood pressure in the leg-a statement on behalf of the British and Irish Hypertension Society. J Hum Hypertens 2020;34(06):418–419
22 Slater J. Validation assessment. Accessed December 7, 2022. https://www.grc.nasa.gov/www/wind/valid/tutorial/valassess.html
23 Pu LLQ. A comprehensive approach to lower extremity free-tissue transfer. Plast Reconstr Surg Glob Open 2017;5(02):e1228
24 Mao H, Xu G. A retrospective study of end-to-side venous anastomosis for free flap in extremity reconstruction. Int J Surg 2015; 17:72–78
25 Lowe GDO. Virchow's triad revisited: abnormal flow. Pathophysiol Haemost Thromb 2003;33(5-6):455–457
26 Jinka SK, Jinka AG, Janis JE. Computational fluid dynamic evaluation of deep inferior epigastric artery perforator (DIEP) flap end-to-side anastomosis. Cureus 2022;14(05):e24650
27 Zhang L, Moskovitz M, Piscatelli S, Longaker MT, Siebert JW. Hemodynamic study of different angled end-to-side anastomoses. Microsurgery 1995;16(02):114–117
28 Sen C, Hasanov A. Comparative geometric analysis of diamond and hole techniques in end-to-side microvascular anastomosis. Microsurgery 2008;28(04):262–264
29 Ooi ASH, Butz DR, Fisher SM, Collier ZJ, Gottlieb LJ. Geometric three-dimensional end-to-side microvascular anastomosis: a simple and reproducible technique. J Reconstr Microsurg 2018; 34(04):258–263
30 Hofer M, Rappitsch G, Perktold K, Trubel W, Schima H. Numerical study of wall mechanics and fluid dynamics in end-to-side anastomoses and correlation to intimal hyperplasia. J Biomech 1996;29(10):1297–1308
31 Harris JR, Seikaly H, Calhoun K, Daugherty E. Effect of diameter of microvascular interposition vein grafts on vessel patency and free flap survival in the rat model. J Otolaryngol 1999;28(03):152–157
32 Monsivais JJ. Microvascular grafts: effect of diameter discrepancy on patency rates. Microsurgery 1990;11(04):285–287
33 Chen HC, Chuang CC, Chen S, Hsu WM, Wei FC. Selection of recipient vessels for free flaps to the distal leg and foot following trauma. Microsurgery 1994;15(05):358–363
34 McCaughan JJ. Successful arterial grafts to the anterior tibial, posterior tibial (below the peroneal), and peroneal arteries. Angiology 1961;12(03):91–94
35 Dardik H, Dardik I, Veith FJ. Exposure of the tibial-peroneal arteries by a single lateral approach. Surgery 1974;75(03): 377–382
36 Burusapat C, Nanasilp T, Kunaphensaeng P, Ruamthanthong A. Effect of atherosclerosis on the lateral circumflex femoral artery and its descending branch: comparative study to nonatherosclerotic risk. Plast Reconstr Surg Glob Open 2016;4(09):e856
37 Wikström J, Hansen T, Johansson L, Ahlström H, Lind L. Lower extremity artery stenosis distribution in an unselected elderly population and its relation to a reduced ankle-brachial index. J Vasc Surg 2009;50(02):330–334
38 Tsai YT, Lin TS. The suitability of end-to-side microvascular anastomosis in free flap transfer for limb reconstruction. Ann Plast Surg 2012;68(02):171–174
39 Pafitanis G, Nicolaides M, O'Connor EF, et al. Microvascular anastomotic arterial coupling: a systematic review. J Plast Reconstr Aesthet Surg 2021;74(06):1286–1302
40 Mücke T, Reeps C, Wolff KD, Mitchell DA, Fichter AM, Scholz M. Objective qualitative and quantitative assessment of blood flow with near-infrared angiography in microvascular anastomoses in the rat model. Microsurgery 2013;33(04):287–296

